

FAILURE OF Al-ALLOY AK 4-1 UNDER CREEP-FATIGUE INTERACTION CONDITIONS

FRANTIŠEK NOVÝ*, PETER PALČEK, MÁRIA CHALUPOVÁ

Department of Materials Engineering, Faculty of Mechanical Engineering, University of Žilina, Univerzitná 1, 010 26 Žilina, Slovak Republic

Received 19 November 2004, accepted 14 October 2005

The mechanism of failure of AK 4-1 aluminium alloy was investigated at the temperature of 543 K under creep-high frequency fatigue (20 kHz) conditions. The minimum creep rate and time to fracture were the main criteria being considered to evaluate creep-fatigue interaction. Due to the effect of the cyclic loading the minimum creep rate slightly increases and time to fracture significantly decreases. The cyclic loading has a significant influence on the total lifetime and fracture mechanism governing the alloy deformation behaviour.

Key words: AK 4-1 aluminium alloy, creep-fatigue interaction, high frequency fatigue, failure mechanisms

1. Introduction

In many cases refractory materials are used at the limits of their properties. A detailed research of high temperature materials has confirmed that even if the primary property of high temperature materials is the creep resistance, the creep rupture strength and the creep strength are not the only proper characteristics for the material at higher temperatures and their evaluation based on this fact is not satisfactory. Long-time loading at higher temperatures cannot cause such structural changes that would negatively impact the operation reliability of a given component. Due to this reason all aspects of combined loading during long-time high temperature operation should be investigated.

So far published works in this topic mainly involve low-cycle fatigue tests at higher temperatures. Low-cycle fatigue tests are characterized by high stress amplitude, very low frequency of loading and low number of cycles to failure.

*corresponding author, e-mail: frantisek.novy@fstroj.utc.sk

The articles dealing with a simultaneous influence of creep and high-cycle fatigue were published only rarely. The high-cycle fatigue is characterized by low stress amplitude, high frequency of loading and high number of cycles to failure.

High-cycle creep-fatigue interaction tests were investigated in various materials, namely in copper (500 °C; 120 Hz) [1, 2], in pure nickel (800 °C; 22 Hz) [1, 2] and in CMSX-3 (900 °C; 100 Hz) [3–5] nickel-base superalloy. In these materials the creep rate and the lifetime were found to increase and decrease, respectively. On the other hand, the deceleration of the creep process caused by the influence of the cyclic part of loading superposition was reported in CMSX-4 single crystals (800 °C; 90 Hz) [6–8]. With the decreasing creep rate, the fracture process is accelerated and the lifetime shortened. In chromium-molybdenum steel 2.25Cr-1Mo (600 °C; 120 Hz) [9, 10], the non-monotonous functional dependence of time to fracture on parameter of cycle asymmetry was recorded.

Similar dependences were reported in AISI 304 (700 °C; 120 Hz) [2, 10, 11] austenitic steel and chromium-molybdenum steel 9Cr-1Mo (600 °C; 120 Hz) [2, 12, 13]. The dependence of minimum creep rate on the parameter of cycle asymmetry had a non-monotonous character, too. In CMSX-3 nickel base superalloy, the influence of loading frequency on creep in the range of 1 to 200 Hz at 900 °C was also investigated [4, 5, 14]. A significant decrease of lifetime and the increase of creep rate in comparison with creep tests at constant loading were observed even at loading frequency of 1 Hz. With increasing frequency up to 100 Hz, the lifetime decreases and the creep rate increases even in a more significant rate. However, with further increase of frequency up to 200 Hz the creep rate and time to fracture remained almost unchanged.

At very high frequencies, which are realized by superimposing of cycling loading using ultrasound only the increase of creep rate and the decrease of lifetime were reported. These dependences were observed e.g. in nickel superalloys (710 ÷ 930 °C; 10 ÷ 19 kHz) [15], in copper (160 ÷ 200 °C; 20 kHz) [16], in VT8 titanium alloys (500 °C; 20 kHz) [16], in VT8 titanium alloy (450 ÷ 525 °C; 20 kHz), in POLDI T 110 titanium alloy (500 °C; 20 kHz) [17] and in EI 268 S steel (480 ÷ 500 °C; 20 kHz) [18].

The objective of this study is to investigate the influence of stress amplitude of superimposed cyclic loading on AK 4-1 aluminium alloy creep resistance under the creep-fatigue conditions at high-frequency loading (270 °C; 20 kHz).

2. Experimental material, testing methods and conditions

The wrought Al-Cu-Mg-Fe-Ni aluminium alloy AK 4-1 was used as the experimental material in this investigation. The chemical composition of the alloy is shown in Table 1. This alloy is used for the production of turbine runners of jet engine air blowers. These parts are machined from heat-treated forgings. The forgings undergo the following heat treatment: solution annealing (530 °C ± 5 °C;

Table 1. Nominal chemical composition of AK 4-1 aluminium alloy [wt.%]

Cu	Mg	Fe	Ni	Ti	Si	Mn	Zn	Cr
2.34	1.49	1.27	1.25	0.07	0.28	0.05	0.01	0.03

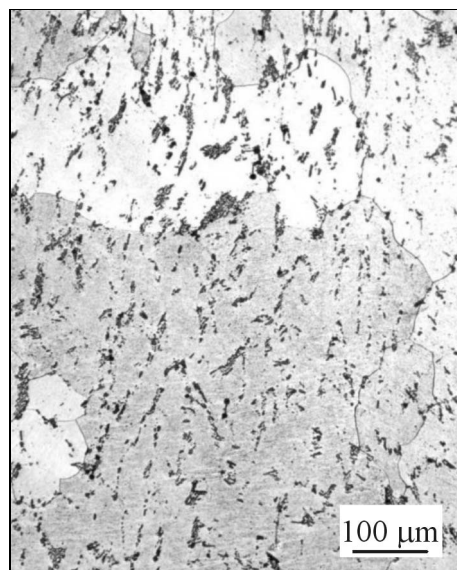


Fig. 1. Microstructure of AK 4-1 Al-alloy after heat treatment. Etching in Dix-Keller.

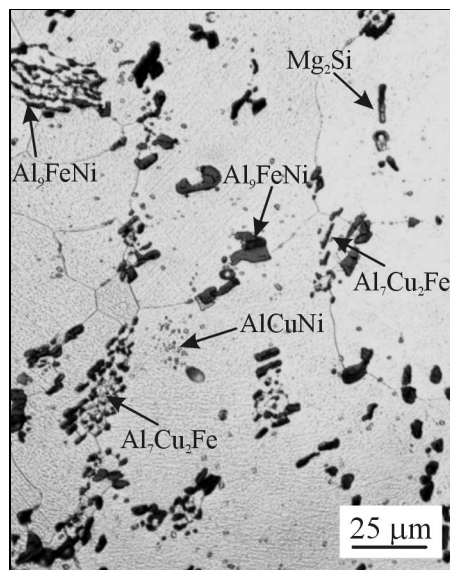


Fig. 2. Microstructure of AK 4-1 Al-alloy after heat treatment. Etching in Dix-Keller.

8 hours), cooling in circulating water ($10 \div 40^\circ\text{C}$; 40 min) and ageing ($190^\circ\text{C} \pm 5^\circ\text{C}$; 10 hours).

The experimental material for all testing specimens was cut off from one turbine runner in the axial direction. In order to relieve the residual stress resulted from machining the machined specimens were annealed at $180 \pm 5^\circ\text{C}$ for 3 hours. The same heat treatment was used after the last machining of the turbine runner. The initial structure of experimental material after forging and heat treatment is shown in Figs. 1, 2. The structure of this alloy after forging differs from casting structure of the same alloy. The casting structure of aluminium alloy AK 4-1 can be seen in [19].

The resistance against creep and fatigue was measured using an AUC-1 testing machine, which was designed at the Department of Materials Engineering, Faculty of Mechanical Engineering, University of Žilina [20]. Due to the enhanced resistance against the oxidation the creep tests at constant loading and creep-fatigue

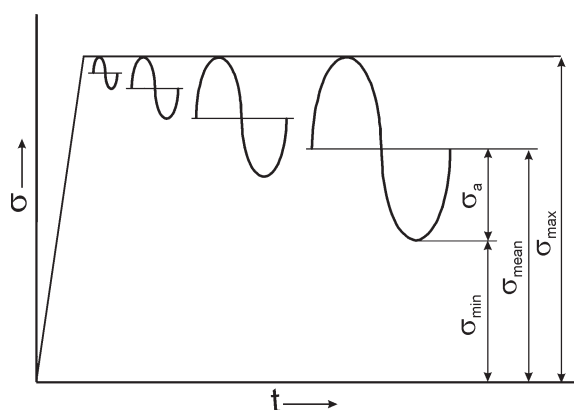


Fig. 3. Scheme of loading schedule.

interaction tests could have been carried out without the protective atmosphere. The testing temperature of 270 °C was stabilized in the range of ± 1 °C. Cylindrical testing specimens of the gauge length of 15 mm and the diameter of 4 mm were used. Superimposed cyclic part of loading had sinusoidal character and the testing frequency was 20100 Hz.

All tests were performed at the constant maximum creep stress $\sigma_{\max} = 140$ MPa. This stress $\sigma_{\max} = 140$ MPa was realized as the sum of the static component σ_{mean} and the cyclic component σ_a (i.e. $\sigma_{\max} = \sigma_{\text{mean}} + \sigma_a$). Five values of σ_{mean} were used, namely 140, 135, 130, 120, 110 MPa. The corresponding values of the cyclic component were 0, 5, 10, 20, 30 MPa (i.e. 140 ± 0 , 135 ± 5 , 130 ± 10 , 120 ± 20 , 110 ± 30) (see. Fig. 3). The following cycle asymmetry parameters $R = \sigma_{\min}/\sigma_{\max} = (1; 0.928; 0.857; 0.714; 0.571)$ correspond to individual tests performed.

3. Results and discussion

3.1 Deformation characteristics at creep-fatigue interaction

The superimposed cyclic loading has only weak influence on shape of creep curves measured at constant loading. On the other hand, the cyclic loading was found to reduce significantly the time to fracture t_f , see Fig. 4. Moreover, the increased superimposed cyclic loading component influenced the relative elongation to fracture ε_f as documented in Fig. 5, where the dependence of time to fracture t_f on the cycle asymmetry parameter R is depicted.

The influence of the cyclic component of loading on the minimum creep rate $\dot{\varepsilon}_m$ is shown in Fig. 6. It is seen that the dependence of the stress amplitude on the

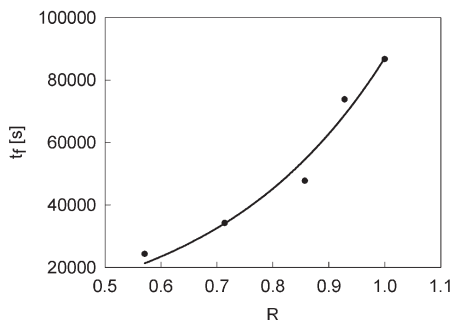


Fig. 4. Dependence of time to fracture t_f vs. R ratio at constant maximum stress in stress cycle $\sigma_{max} = 140$ MPa ($T = 270^\circ\text{C}$, $R = 1; 0.928; 0.857; 0.714; 0.571$).

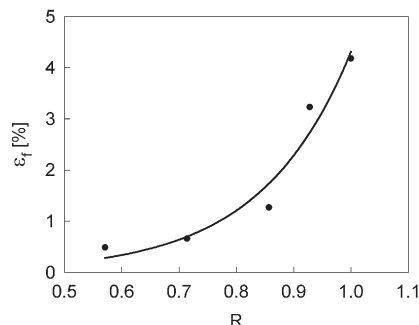


Fig. 5. Dependence of relative elongation to fracture ϵ_f vs. R ratio at constant maximum stress in stress cycle $\sigma_{max} = 140$ MPa ($T = 270^\circ\text{C}$, $R = 1; 0.928; 0.857; 0.714; 0.571$).

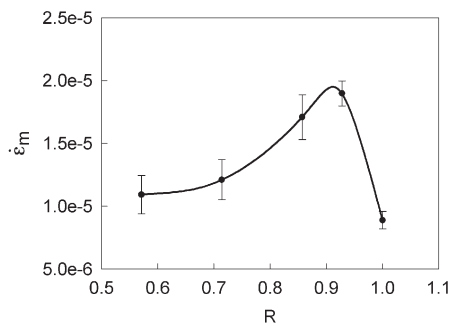


Fig. 6. Dependence of minimal creep rate $\dot{\epsilon}_m$ vs. R ratio at constant maximum stress in stress cycle $\sigma_{max} = 140$ MPa ($T = 270^\circ\text{C}$, $R = 1; 0.928; 0.857; 0.714; 0.571$).

minimum creep rate is non-monotonous, i.e. initially increases, reaches a maximum and then steeply decreases, when R approaches to 1. This surprising synergic effect depends probably strongly on frequency. The temperature and stress dependence of this synergic effect was confirmed in [21] as well.

3.2 Fracture analysis

The SEM analysis was performed on crept specimens and specimens subjected to various cyclic loading components occurring during combined creep-fatigue tests. The fracture analysis was done using TESLA BS 343 scanning electron microscope operating at 15 kV.

Neck formation was not observed at any of the crept specimens. An extensive network of cracks was formed on the surface as seen in Fig. 7. The fracture morpho-

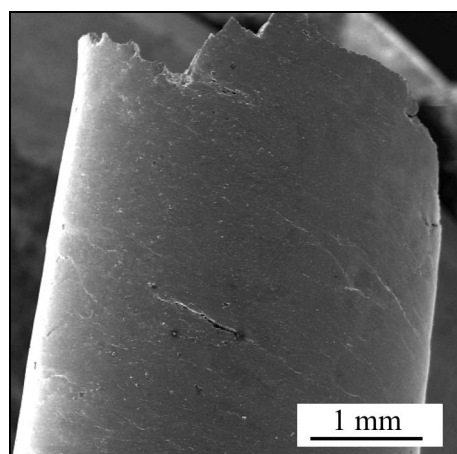


Fig. 7. Cracks on the surface of crept specimen ($\sigma = 140$ MPa, 270°C).

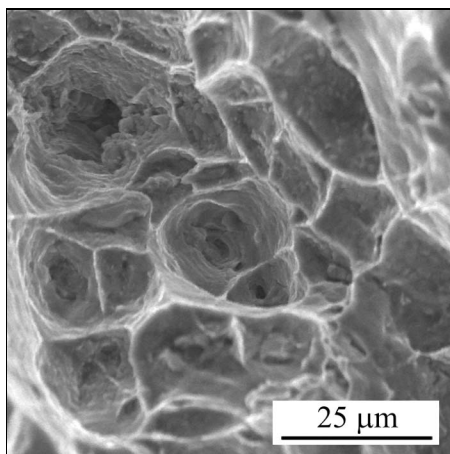


Fig. 8. Cavities on the fracture surface of crept specimen ($\sigma = 140$ MPa, 270°C).

logy strongly depends on the applied testing conditions. Transgranular failure with clear dimple morphology and cavity occurrence was found at all fracture surfaces subjected to static creep only. Fracture surfaces were covered by particles of intermetallic phases or their parts embedded in the matrix. The size of these particles was in the range 0.5 to $15 \mu\text{m}$. The fracture was governed by cavity formation (Fig. 8) due to the activity of creep mechanisms.

The character of fracture surface depends significantly on the amplitude of cyclic loading. The appearance of the fracture surface upon the application of any even very small amplitude of superimposed cyclic loading ($\sigma_a = 3.6\%$ of σ_{\max}) on creep stress was completely different from that of the creep test only. At all crept specimens a transgranular ductile fracture with dimple morphology, originated as a result of cavity merging, was observed. On the other hand, the fracture morphology of specimens, which underwent combined creep-fatigue loading was changed to transgranular fatigue failure character with the occurrence of cavities. This type of fracture was observed at all specimens, which were tested under combined creep-fatigue loading.

Both at the creep tests performed at constant loading and combined creep-fatigue tests the failure process was not accompanied by neck formation, and the surficial intergranular cracks originated and developed as a consequence of the failure created by grain boundary cavity formation (Fig. 9). Unlike creep tests after combined creep-fatigue tests the size of the surficial intergranular cavities was smaller, and their number along the cavitated boundaries was much higher.

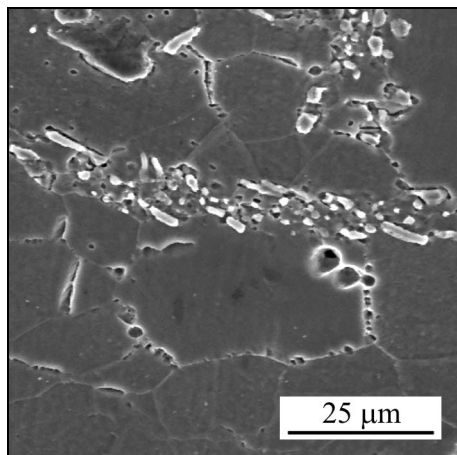


Fig. 9. Micrograph of cavities on the surface of the specimen after creep-fatigue interaction test ($\sigma = 110 \pm 30$ MPa, 270°C).

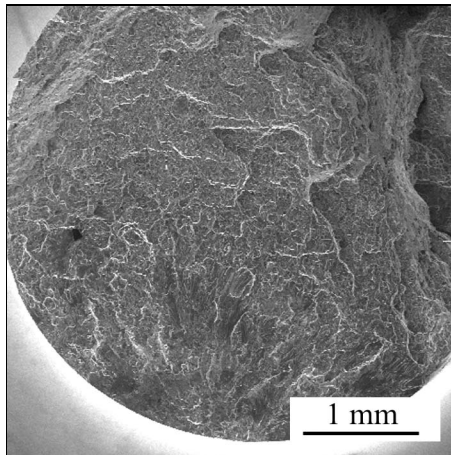


Fig. 10. Fracture surface after creep-fatigue interaction test ($\sigma = 110 \pm 30$ MPa, 270°C).

A magistral crack was initiated by merging of shallow surfacial intergranular cracks. Due to fatigue mechanisms the initiated fatigue crack grew transgranularly in the perpendicular direction to the direction of loading (Fig. 10).

The fatigue crack grew through the cross-section of the specimen and no secondary cracks were observed. During the stable growth of fatigue crack, the fracture has a transgranular character with clear facets joined by steps. The width of facets and the depth of steps depend on the cycle asymmetry parameter R . The widest facets were formed if the applied cyclic part of loading had the lowest amplitude (Fig. 11).

The fracture surfaces created by facets consist of steps having an atypical appearance reminding fans or rivers. This type of fracture is similar to cleavage fatigue fracture with river morphology, which is created by cumulation of fatigue failure in front of the fatigue crack front. However, a magnified image of these facets indicates that the fracture mode is in fact a transgranular ductile fatigue fracture formed by striation mechanism (Fig. 12).

The width of facets decreased with increasing amplitude of cyclic loading (Figs. 13, 14) and the striation became sharper and bigger. The fatigue striations on the investigated fracture surfaces had a regular spacing that depends on the distance between the investigated zone and the place of crack initiation. The striation spacing increased with increasing length of the fatigue crack because of the increased stress intensity factor at the crack front. Due to the circular cross-section of test specimens no unambiguous conclusions about the rate of fatigue crack growth

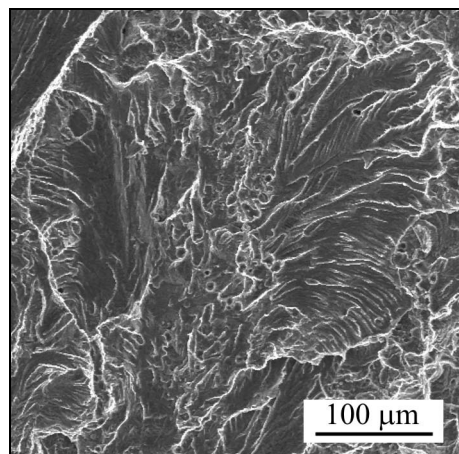


Fig. 11. Transgranular fatigue fracture with sharp facets ($\sigma = 135 \pm 5$ MPa, 270 °C).

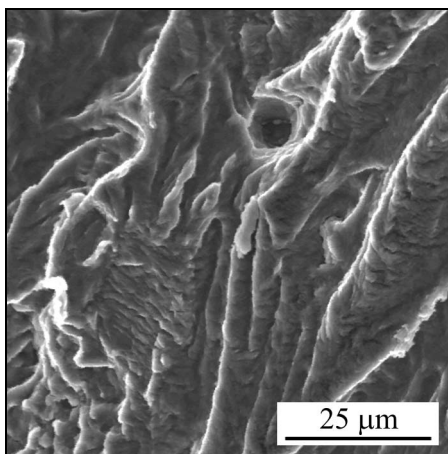


Fig. 12. Detail of fatigue fracture ($\sigma = 135 \pm 5$ MPa, 270 °C).

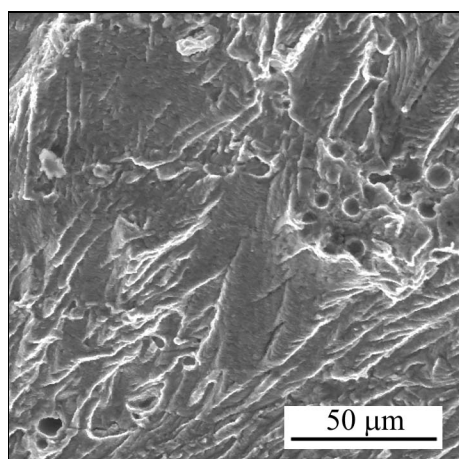


Fig. 13. Transgranular fatigue fracture with local cavities distribution ($\sigma = 110 \pm 30$ MPa, 270 °C).

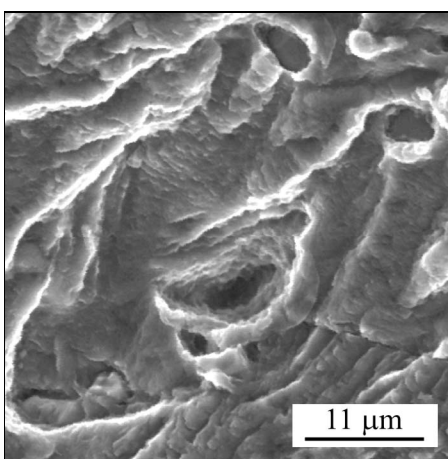


Fig. 14. The cavity appearance on the fatigue fracture surface ($\sigma = 110 \pm 30$ MPa, 270 °C).

may be drawn. The striations in individual areas change very often their direction with respect to the magistral crack.

The activity of cavity mechanisms (playing an important role in the failure

at the creep tests at constant loading) was during combined creep-fatigue tests much lower than during the creep tests. The creation of cavity is a time dependent process, which is obviously much shorter during combined creep-fatigue tests. The shorter time, which is available for the cavity formation during creep-fatigue tests, may explain their smaller sizes observed on fracture surfaces of specimens after creep-fatigue tests. SEM observation confirmed the low density and small size of cavities at fracture surfaces of all specimens after creep-fatigue tests (Figs. 13, 14).

4. Conclusion

From the experimental results obtained from this investigation the following conclusions can be drawn:

- The cyclic loading has no influence on the primary creep, but it has a significant influence on the secondary and tertiary creep.
- The introduction of the cyclic loading at the creep-fatigue tests increases the minimal creep rate. The dependence of $\dot{\epsilon}_m$ on R has a non-monotonous character.
- On the other hand, the introduction of the cyclic component of loading reduces the time to fracture as well as the relative elongation to fracture.
- The fractography analysis of fracture surfaces shows that at creep-fatigue tests the fracture character changes even at very low amplitude of cyclic loading. Transgranular ductile fracture with dimple morphology characterized by high density of cavities (size $15 \div 25 \mu\text{m}$) at creep tests has changed to transgranular fatigue fracture with lower density of cavities having a size of approximately $5 \mu\text{m}$ at creep-fatigue tests.

Acknowledgements

The paper is dedicated to Prof. RNDr. Pavel Lukáč, DrSc., Dr.h.c., at the occasion of his 70th birthday.

This work has been supported by the Scientific Grant Agency of the Ministry of Education and Slovak Academy of Sciences, SR, grant No. 1/10282/03.

The part of the results of this work was supported by the founding from the state program of research and development – New materials and technologies in the construction of machines and equipment, thematic state program “The Development of Personality and Talent of Young Employees and Doctorates of Research and Development under 35 years.”

REFERENCES

- [1] SKLENIČKA, V.: In: METALLOGRAPHY '94. Ed.: Hrivňák, I. Košice, HF TU Košice 1994, p. 93.
- [2] LUKÁŠ, P.—KUNZ, L.—SKLENIČKA, V.: In: Strength of Materials. Proc. ICSMA – 10. Ed.: Oikawa, H. Sendai, The Japan Institute of Metals 1994, p. 17.
- [3] ZRNÍK, J.—HORŇAK, P.—ŽITŇANSKÝ, M.—WANG, J.—YONGSI, Y.—WANG, Z. G.: Kovine, zlitine, technologije, 30, 1996, p. 179.
- [4] ZRNÍK, J.—WANG, J. A.—YU, Y.—PEJING, L.—HORŇAK, P.: Mat. Sci. Eng., A 234–236, 1997, p. 884.

- [5] ZRNÍK, J.—HORŇAK, P.—ŽITŇANSKÝ, M.: In: Metallography '98. Ed.: Hrivňák, I. Košice, HF TU Košice 1998, p. 256.
- [6] KUNZ, L.—LUKÁŠ, P.: In: Degradácia vlastností konštrukčných materiálov únavou. Ed.: Puškár, A. Žilina, Sjf VŠDS v Žiline 1995, p. 46.
- [7] LUKÁŠ, P.—KUNZ, L.—SVOBODA, J.: Mat. Sci. Eng., A 234–236, 1997, p. 459.
- [8] LUKÁŠ, P.—KUNZ, L.: Mat. Sci. Eng., A 214, 1996, p. 167.
- [9] KUNZ, L.—LUKÁŠ, P.—SKLENIČKA, V.: Kovove Mater., 31, 1993, p. 76.
- [10] LUKÁŠ, P.—KUNZ, L.—SKLENIČKA, V.: Mat. Sci. Eng., A 129, 1990, p. 249.
- [11] LUKÁŠ, P.—KUNZ, L.—SKLENIČKA, V.: Kovove Mater., 29, 1991, p. 64.
- [12] VAŠINA, R.—LUKÁŠ, P.—KUNZ, L.—SKLENIČKA, V.: Fatigue Fract. Eng. Mater. Struct., 18, 1995, p. 27.
- [13] KUNZ, L.—LUKÁŠ, P.—SKLENIČKA, V.: Materials for Advanced Power Engineering. Part I. Dordrecht, Kluwer Academic 1994.
- [14] ZRNÍK, J.—WANG, J. A.—YU, Y.—HORŇAK, P.: In: Degradácia vlastností konštrukčných materiálov únavou. Ed.: Bokůvka, O. Žilina, ŽU v Žiline 1997, p. 76.
- [15] SHEFFLER, K. D.: Metall. Trans., 3, 1972, p. 167.
- [16] JANOUŠEK, M.—MÍŠKUFOVÁ, D.: In: Degradácia vlastností konštrukčných materiálov únavou. Ed.: Puškár, A. Žilina, SET VŠDS Žilina 1991, p. 111.
- [17] JANOUŠEK, M.: Synergické působení creepu a únavy na titanovou slitinu VT 8. [Kandidátska dizertačná práca]. Žilina, Sjf VŠDS Žilina 1992.
- [18] PUŠKÁR, A.—ŠUFLIARSKY, P.: Kovove Mater., 35, 1997, p. 382.
- [19] PELACHOVÁ, T.—LAPIN, J.: Kovove Mater., 37, 1999, p. 399.
- [20] PUŠKÁR, A.—PALČEK, P.—MEŠKO, J.: Zariadenie pre súčasné hodnotenie odolnosti telies proti únave a tečeniu. ZN č. 384/89, Žilina, VŠDS Žilina 1989.
- [21] NOVÝ, F.: Interakcia tečenia a únavového zaťaženia zliatiny AK 4-1č. [Dizertačná práca]. Žilina, Sjf ŽU Žilina 2002.